The water-equivalence of phantom materials for $^{90}Sr-^{90}Y$ beta particles

Lesley A. Buckley,[a] Bruce R. Thomadsen, and Larry A. DeWerd
University of Wisconsin, Department of Medical Physics, 1530 Medical Sciences Center, Madison, Wisconsin 53706

(Received 15 August 2000; accepted for publication 9 April 2001)

Intravascular brachytherapy requires that the dose be specified within millimeters of the source. High dose gradients near brachytherapy sources require that the source-detector distance be accurately known for dosimetry purposes. Solid phantoms can be designed to accommodate these stringent requirements. This study reports dosimeter readings from $^{90}Sr-^{90}Y$ sources measured in water, A150, polystyrene and in an epoxy-based water-equivalent plastic. Measurements showed that while A150 and the epoxy-based plastic agreed well with water when the surface of the source contacted the detector housing, the relative response in the phantoms decreased with increasing depth in phantom, falling to ~0.55 those of water at a depth of 5 mm. Readings in polystyrene were within 4% of those in water between 1 and 2 mm depth. However, while polystyrene followed water more closely than the other two materials, at greater depths the relative response in polystyrene to water varied from 0.65 to 1.34. When the density of the materials is accounted for, the relative response in A150 is nearly constant with increasing areal density. Furthermore, the response in A150 shows the closest agreement with that in water of any of the solid materials for higher areal densities. For values below 0.3 g/cm^2, polystyrene shows the closest agreement with water. © *2001 American Association of Physicists in Medicine.* [DOI: 10.1118/1.1376176]

Key words: beta particles, dose gradient, intravascular brachytherapy, restenosis, strontium-90

INTRODUCTION

Angioplasty is commonly used in place of bypass surgery to treat coronary artery disease. Despite causing fewer major complications than bypass surgery, a serious limitation of angioplasty is the occurrence of restenosis in approximately 35%–40% of patients.[1] Restenosis reduces blood circulation and oxygen flow through the artery, necessitating additional treatment. Evidence suggests that irradiation of the vessel walls may significantly lower the risk of developing restenosis following angioplasty.[2] Intravascular brachytherapy may be used for this purpose.

Unlike traditional brachytherapy, where the dose is typically specified at distances on the order of 1 cm from the source, the dose distribution must be known on the order of millimeters for intravascular brachytherapy.[3] Due to the high dose gradients near brachytherapy sources, combined with the need to specify the dose within millimeters of the source, the source-detector distance must be specified very accurately for dosimetry measurements. This is facilitated by the use of solid phantoms since they can be machined precisely to yield an accurate and reproducible source-detector geometry. Since water is the ideal reference material for dosimetry measurements, the choice of a solid to be used for such a phantom depends largely on whether the material is a suitable dosimetric substitute for water when using the given type of radiation. A number of authors have studied the dosimetric characteristics of materials for photon-emitting brachytherapy sources,[4,5] however, no such information is available for beta-emitting sources. Since beta sources have been proposed for use in intravascular procedures,[6] accurate dosimetry of these sources is critical. This requires the identification of solid phantom materials that would be suitable for this purpose. Initial work on these materials was presented at the 1998 Advances in Cardiovascular Radiation Therapy conference.[7] This study compares readings on radiation detectors exposed to beta particles from $^{90}Sr-^{90}Y$ sources in three solid materials and in water.

MATERIALS AND METHODS

Source description

The study reported here was performed using two different $^{90}Sr-^{90}Y$ sources. The first source was a flat-faced 5.1 mCi $^{90}Sr-^{90}Y$ source. The source material was plated on the flat end surface of a stainless steel cylinder 10.5 mm long and 2.3 mm in diameter. The mean and maximum beta particle energies are 0.8 and 2.3 MeV, respectively. The source was highly directional and was used in this study with the active face directed towards the detectors. The second type of source was the Novoste Beta-Cath™ System (Novoste Corporation, Norcross, GA). This system consists of a source train containing twelve cylindrical $^{90}Sr-^{90}Y$ pellets aligned in a plastic catheter such that the total active length of the train is 3 cm. The two source geometries are shown in Fig. 1.

Detectors

The measurements were performed using two types of detectors: A PTW (model 31006) pinpoint ionization chamber and a PTW (model 60003) diamond detector (PTW-Freiburg, Germany). The physical characteristics of the detectors are summarized in Table I. Each of the detectors has a small sensitive volume to provide good spatial resolution.

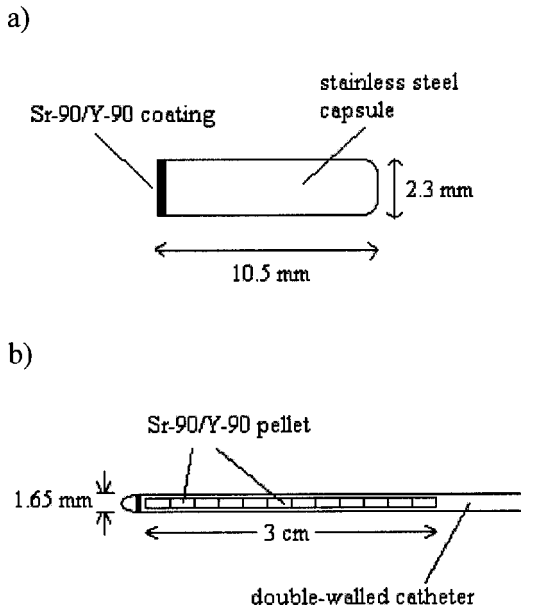

FIG. 1. Source geometry for (a) the flat-faced source and for (b) the source train.

Each detector is waterproof so that no additional waterproofing sleeve is required. This reduces the uncertainty in the positioning of the detector. The pinpoint chamber has a cylindrical geometry and the long axis of the chamber was oriented perpendicular to the long axis of the flat-faced source and parallel to the source train catheter. The diamond detector has a wafer-shaped sensitive volume at the end of and perpendicular to the cylindrical housing, and the housing was oriented parallel to the flat-faced source and perpendicular to the source train catheter. The central electrode of the pinpoint chamber is 1.6 mm from the outer surface and the position of the sensitive volume in the diamond detector is 1 mm from the surface.[8] Unlike the pinpoint chamber, the diamond detector does not require temperature and pressure corrections and has very little energy dependence.[8,9]

Phantom materials

This study investigated the properties of A150 plastic (Exradin, Lisle IL), Virtual Water™ (MED-CAL INC., WI) and polystyrene when used with beta particles. The Virtual Water is an epoxy-based water substitute equivalent to Solid Water™ (Gammex-RMI, Middleton WI). It was studied since it is a commonly used dosimetric phantom material. A150 plastic is of interest since it is the phantom material used during the calibration of beta emitting brachytherapy sources at the National Institute of Standards and Technology.[10] Polystyrene is a third material that is often used for solid phantoms and preliminary studies suggested that it may be better suited to substitute for water in the dosimetry of beta sources.[7] The detector response to beta particles in each material was compared to those in water. Table II shows the measured densities of the three solid materials.

TABLE I. Detector specifications.

Detector	Sensitive volume	Operating bias	Sensitivity to ^{60}Co
Pinpoint chamber	0.015 cm^3	+300	4×10^{-10} C/Gy
Diamond detector	0.002 cm^3	+50	3×10^{-7} C/Gy

TABLE II. Densities of the phantom materials, measured at 24 °C.

A150	1.1464 g/cm^3
Virtual Water	1.0467 g/cm^3
Polystyrene	1.0393 g/cm^3

A schematic of the phantom design is shown in Fig. 2. Each phantom consists of three carefully machined segments: a source block, a detector block, and a set of intervening slabs. The source block is a uniform block of the material machined with a single hole to accommodate the flat-faced source and position it so that the active face of the source lies centrally in the plane of the block surface. The opposing side of the source block has a slot spanning the width of the block in which the source train catheter can be positioned. The source block can be oriented with either source holder facing the detector block depending upon which source is to be used. The detector block has two slots; each designed to accommodate a different detector. The slots are machined such that when the source and detector blocks are held together the sensitive volume of the detector is centered over the source in the desired orientation. In this configuration, the dimensions of the phantoms are large enough so that the central location of the source ensures that all of the beta radiation is contained within the phantom. Two plugs were machined to fill the detector slot not in use. To accommodate the tapered design of the pinpoint chamber, a cap was machined out of each solid material to fit over the sensitive volume of the chamber such that it would lie flat in the phantom block. All of the components were machined to

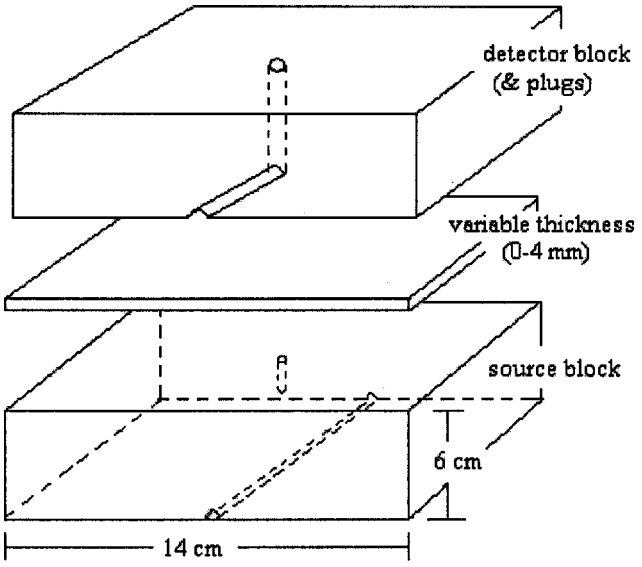

FIG. 2. Schematic of the solid phantom design.

minimize air gaps within the phantom. The intervening slabs are of varying thicknesses and are used to increment the source-to-detector distance by 1 mm steps between 1 and 5 mm.

Measurements were taken of the detector current at varying source-detector separations within the phantom to give a value $I_p(d)$ in Amperes, where d is the source-detector distance and the subscript p refers to the measurement phantom material. The measurements were compared to equivalent readings $I_w(d)$ taken at varying distances in a water tank. The ratios of the readings I_p/I_w at a given d value were used to evaluate the relative effect of each material on the radiation. The source detector distance was varied so that the effect of depth on the ratio I_p/I_w could be evaluated.

Water measurements

The measurements in water were performed using an Accuscan2™ water tank (Dynamic Design & Development, CA). The source was held in position by a stationary support within the tank. The detector was affixed to a computer controlled scanning arm such that the source-detector distance could be varied between 1 and 5 mm. The source-detector distance was incremented by 1 mm steps to correspond to equivalent readings taken in the solid phantoms.

RESULTS

Detector effects

The two detectors pose very different geometries relative to the source and illustrate the effects of detector geometry. This point is crucial when considering the dosimetry of beta-emitting sources since the exact source-detector geometry significantly impacts the dosimetry results. This issue motivates the use of two different detectors.

The response of the detectors to the beta radiation in each of the phantom materials is shown in Fig. 3 for the flat-faced ^{90}Sr–^{90}Y source. The source-detector distance is the distance between the source surface and the effective point of measurement within the detector. The readings from the pinpoint chamber have been corrected using the Kondo–Randolph correction factor[11] such that effective point of measurement is at the central electrode. The source-detector distances for the data points using the pinpoint chamber in the solid phantoms are determined by the thickness of the cap that covered the sensitive volume of the chamber in addition to the thickness of the intervening slabs of material.

The data points shown in Fig. 3 are the average values of current readings from multiple data sets. The standard deviation of the readings at a single distance due to fluctuations in the electrometer reading was ~0.5%. In order to evaluate the reproducibility of each of the source-detector geometries, the results from independent data sets were compared. The experimental uncertainty for the data points in Fig. 3 is shown in Fig. 4 as the percent standard deviation of the current readings from independent data sets.

Since the depth of the sensitive volume within the detector housing is different for each of the two detectors, the data

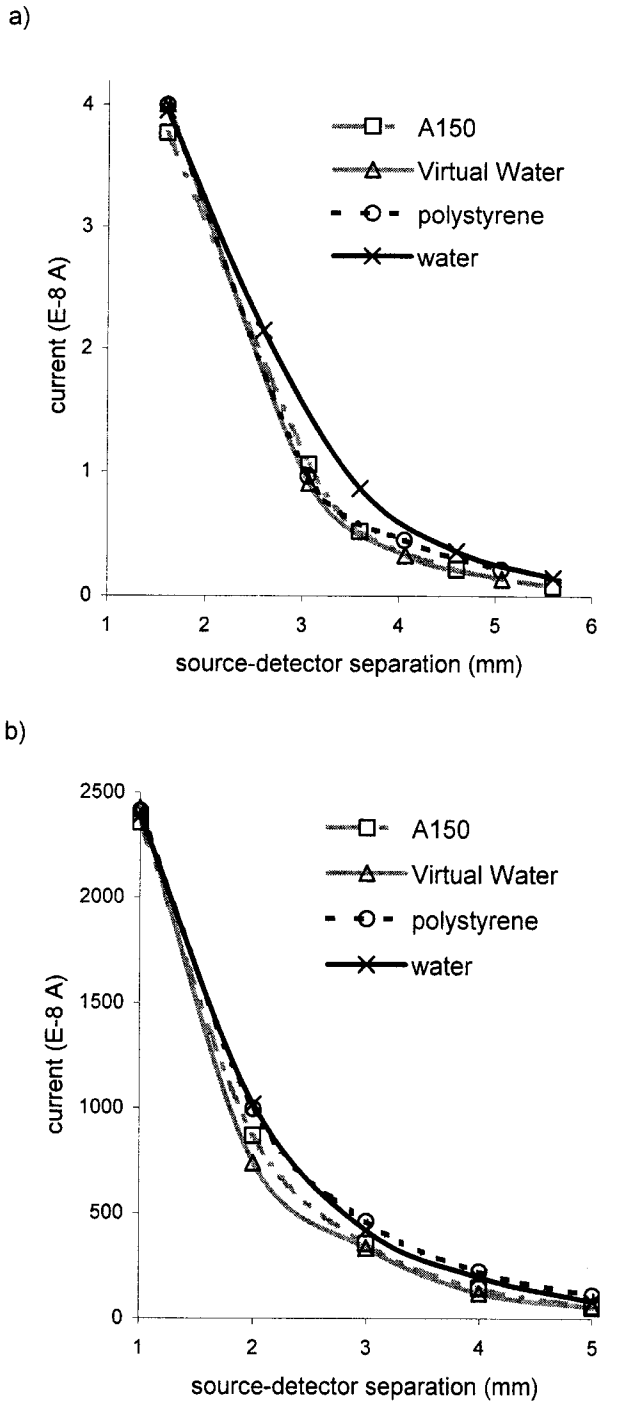

FIG. 3. Current readings at varying depths in phantom materials using the flat-faced source with; (a) the pinpoint chamber and; (b) the diamond detector.

points from the pinpoint chamber have been interpolated to determine relative responses at a set of distances common to the diamond detector. Figure 5 shows the values of I_p/I_w for all of the phantom materials and with each of the detectors when used with the flat-faced source. Both detectors show a decrease in the I_p/I_w value with increasing depth in both A150 and Virtual Water. The behaviors of the detectors differ in polystyrene, however, with the diamond detector showing a nearly continuous increase in I_{poly}/I_w with depth

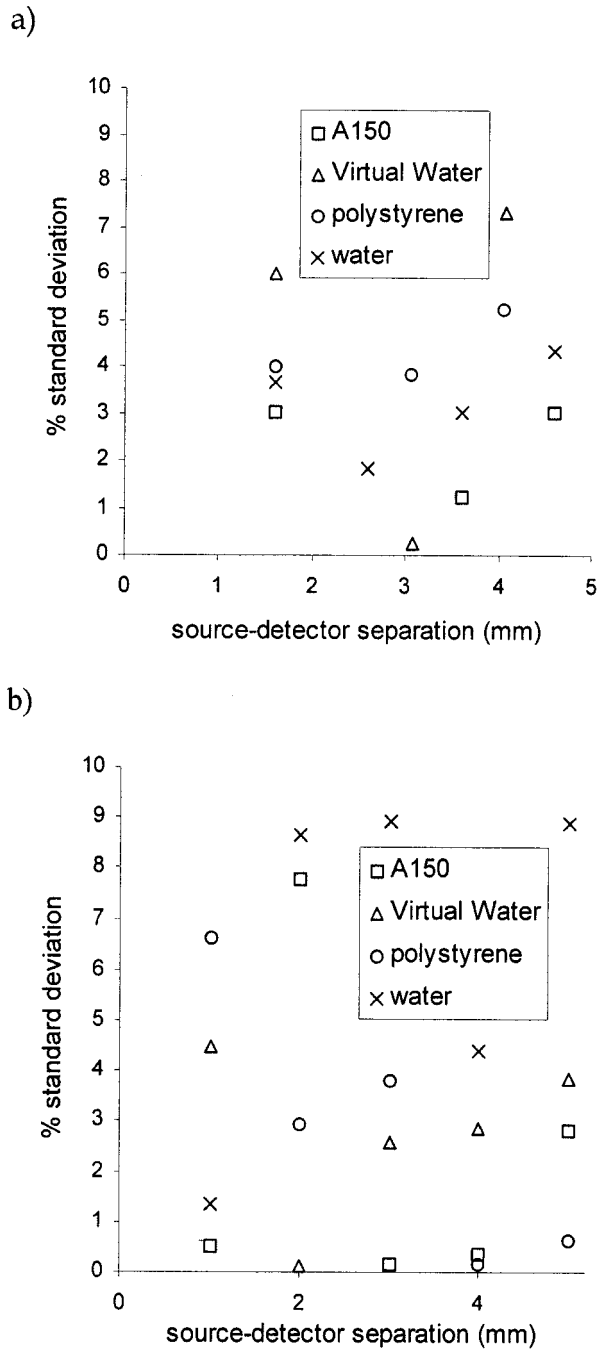

FIG. 4. Standard deviation of current readings from independent data sets expressed as a percentage of the mean using the flat-faced source with; (a) the pinpoint chamber and; (b) the diamond detector.

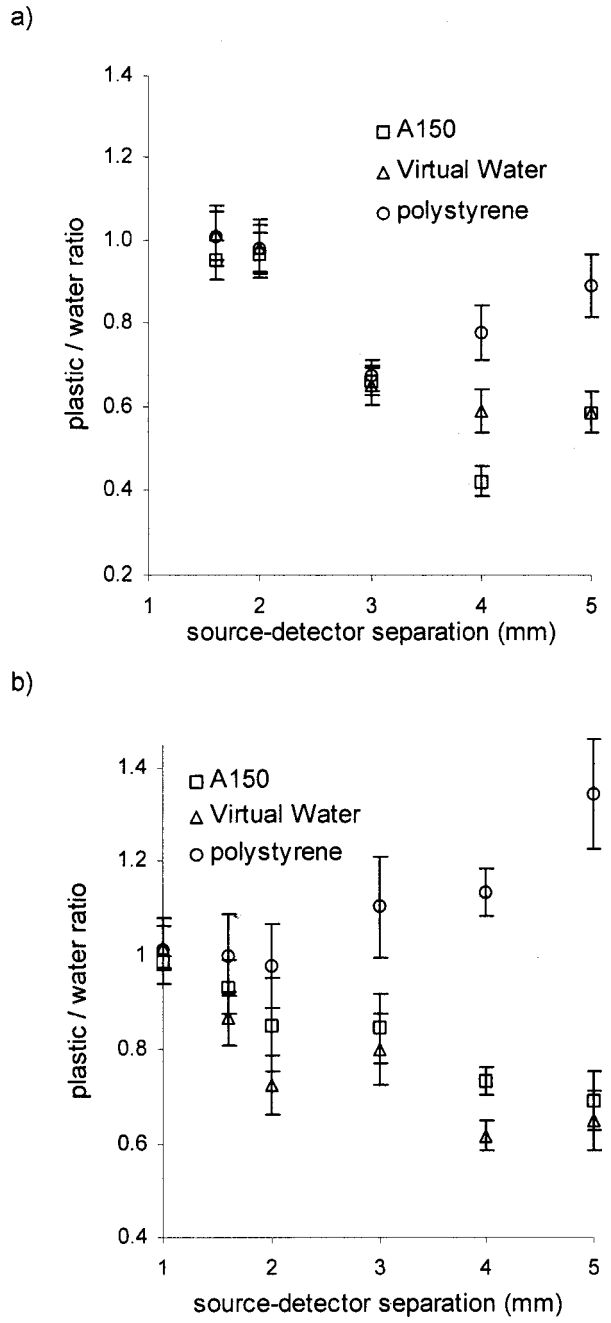

FIG. 5. Response in plastic phantoms relative to water using; (a) the pinpoint chamber and; (b) the diamond detector. Data is shown for the flat-faced source.

and the pinpoint chamber showing an initial decrease in the ratio with increasing in depth. The error bars in Fig. 5 were computed using a partial derivative expansion of I_p/I_w in the variables I_p and I_w and with the uncertainties in I_p and I_w as described above and shown in Fig. 4.

Comparison of the results obtained with the two detectors is shown in Fig. 6. The ratio of the pinpoint chamber result to the diamond detector result is plotted for all source-detector separations. At small source-detector distances, the pinpoint chamber yields ratios that are greater than the ratios from the diamond detector. At higher source-detector separations, the phantom to water ratios obtained with the pinpoint chamber are consistently lower than those from the diamond detector.

Response with source geometry

As discussed previously, the source-detector geometry is crucial for beta particle dosimetry and small changes in this geometry can impact significantly on the results. Using a second source geometry enables the comparison of the results obtained in two different arrangements. Figure 7 shows

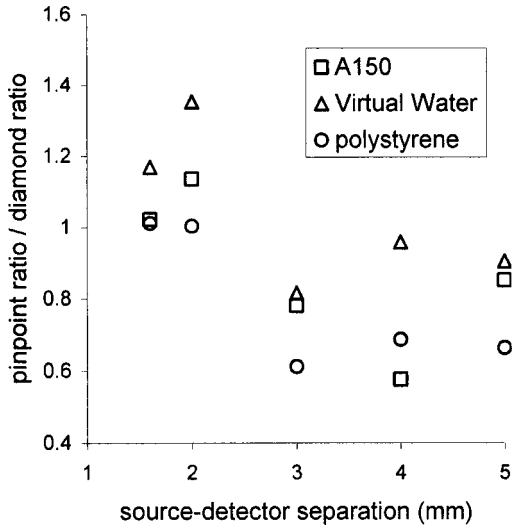

FIG. 6. Ratios of results obtained with the two detectors for the flat-faced source. The ratio is presented as the ratio of the result from the pinpoint chamber over the result from the diamond detector.

the ratios I_p/I_w for each of the phantom materials at varying source-detector separations using the source train. This data is shown for the diamond detector and is analogous to Fig. 5(b), which was obtained using the flat-faced source.

Material comparison

The three solid materials were compared to water for their attenuation and scatter properties. Ideally, a substitute material for water should yield ratios of I_p/I_w near 1.00. From Figs. 5 and 7 it is clear that none of the materials have characteristics similar to water for beta particles over all phantom depths. All three materials show close agreement with water when the source was in contact with the detector

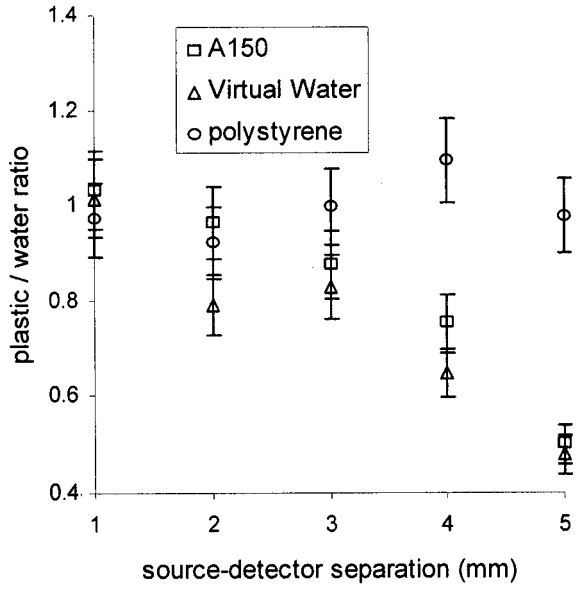

FIG. 7. Response in plastic phantoms relative to water using the Novoste Beta-Cath™ system with the diamond detector.

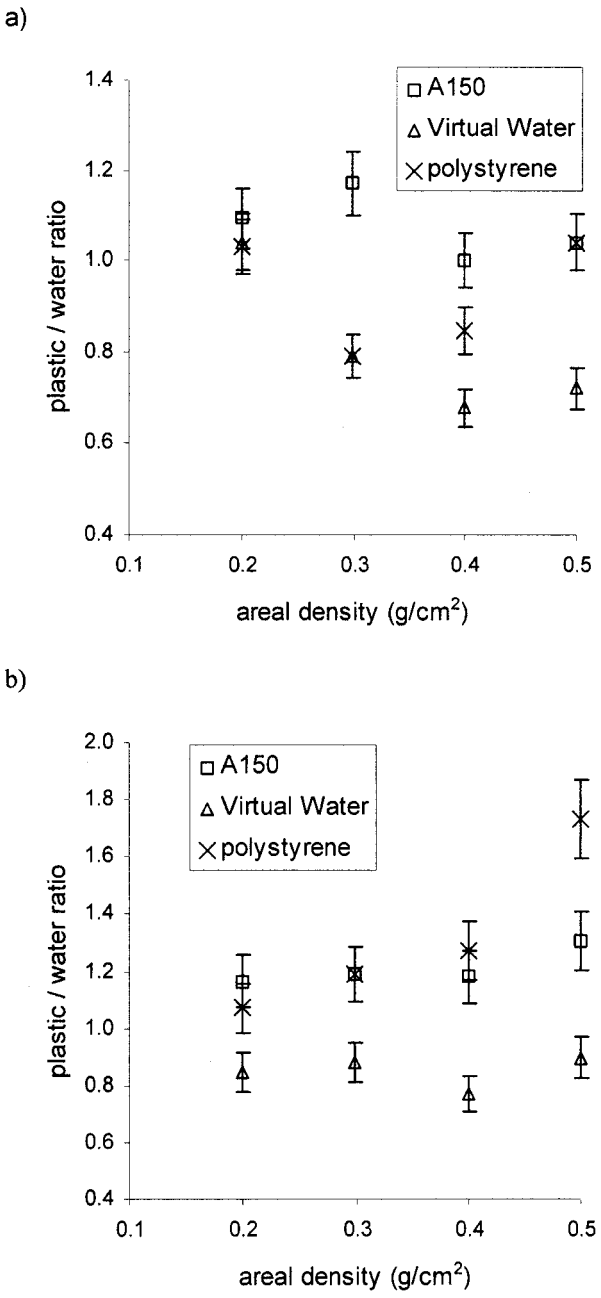

FIG. 8. Response in plastic phantoms relative to water plotted against areal density for (a) the pinpoint chamber and; (b) the diamond detector using the flat-faced source.

housing. This occurs at 1 and 1.6 mm for the diamond detector and pinpoint chamber, respectively. The relative responses at these positions give an indication of the scatter properties of the solid material relative to water since there is no intervening material and the only difference in the readings will come from the scatter from the surrounding medium. At these positions, the responses in the three solids agree within a few percent of those in water, indicating that the scatter characteristics are similar for all of the materials.

When the source was not in contact with the detector housing the ratio I_p/I_w deviated from 1.0 for all of the materials. The value of I_p/I_w for A150 decreased from 0.93 to

0.5 between 1.6 and 5 mm. Virtual Water showed similar behavior, with ratios decreasing over the same distances from 0.92 to 0.56. The relative response in polystyrene did not show the same behavior as the other two solids at depth and at all source-detector distances polystyrene followed water more closely than did the other two materials. This was true for both detectors and for both source geometries. For polystyrene between 1.6 and 5 mm, I_{poly}/I_w was in the range 0.65–1.34 when using the flat-faced source. The results for polystyrene using the source train showed less variation and the ratio I_{poly}/I_w varied between 0.95 and 1.10 over the range of distances used. At depths below 2 mm, the response of the detectors in polystyrene was within 4% of that in water in all source and detector geometries.

An alternate way to compare the detector responses in the solid phantoms to those in water is to account for the differences in the densities of the materials. This is achieved by multiplying the source-detector separation by the density of the material given in Table II to yield the areal density in units of g/cm^2. Figure 8 shows the values of I_p/I_w plotted against areal density for all of the solid phantom materials. When the results are adjusted for the density, the response in A150 shows greater agreement with that in water than do the responses in the other two materials. The relative response obtained in A150 to that obtained in water was nearly constant with areal density for all values below 0.4 g/cm^2. Both Virtual Water and A150 follow water more closely with the density dependence removed than when they are compared to water on a purely geometric basis. The density of polystyrene is closest to that of water of the three phantom materials, so the results in polystyrene are affected the least by the removal of the density dependence. At areal densities below 0.3 g/cm^2 polystyrene still shows the best agreement with water, however, at larger values the response varies significantly from that of water.

DISCUSSION AND CONCLUSIONS

Though water is the ideal dosimetric phantom material, convenience and geometric considerations often dictate the need for solid phantom materials. The experiment reported by Thomadsen *et al.*[7] measured transmission through sheets of solid materials surrounded by water and found that polystyrene gave the best agreement to measurements performed with only water (a ratio of 1.0). Their experimental geometry avoided the backscatter from the polystyrene, looking only at transmission.

The responses to beta particles in A150 plastic and Virtual Water reported here show that neither solid material is water-equivalent for the dosimetry of ^{90}Sr–^{90}Y sources. Though both materials show close agreement with water at the source surface, the relative responses of radiation detectors within each of the materials decrease significantly compared with water with depth in the phantom. Readings in polystyrene are closer to those in water than the other two materials. Between 1 and 2 mm from the source, the detector response in polystyrene is within 4% of that in water, however, the relative response can vary by as much as 30% at greater depths.

If the density of the materials is accounted for by considering the areal density in place of the geometric distance, polystyrene still follows water more closely than the other two materials for areal densities below 0.3 g/cm^2. A150 shows a more consistent relative response with increasing areal density and more closely mimics water at larger areal density values than do the other two materials. However, the relative response in A150 to water varies between 10% and 20% and it should again be stressed that the results presented here show that none of the phantom materials are water-equivalent for the dosimetry of ^{90}Sr–^{90}Y beta particles. Furthermore, the use of areal density in place of distance must be regarded with caution. While it may be advantageous to account for the density of the phantom material, the use of areal density in place of distance no longer permits the use of a straightforward geometry function (or similar concept). If the phantom material is intended to be used as a replacement for water, with no corrections applied, then the geometric distance and not the areal density should be used.

[a]Electronic mail: labuckley@students.wisc.edu

[1] S. J. Pocock *et al.*, ''Meta analysis of randomized trials comparing coronary angioplasty with bypass surgery,'' Lancet **346**, 1184–1189 (1995).
[2] R. Waksman, ''Radiation for prevention of restenosis: where are we?,'' Int. J. Radiat. Oncol., Biol., Phys. **36**, 959–961 (1996).
[3] H. I. Amols, ''Dosimetric considerations for catheter- based beta and gamma emitters in the therapy of neointimal hyperplasia in human coronary arteries,'' Int. J. Radiat. Oncol., Biol., Phys. **36**, 913–921 (1996).
[4] A. S. Meigooni, Z. Li, V. Mishra, and J. F. Williamson, ''A comparative study of dosimetric properties of plastic water and solid water in brachytherapy applications,'' Med. Phys. **21**, 1983–1987 (1994).
[5] A. S. Meigooni, J. A. Meli, and R. Nath, ''A comparison of solid phantoms with water for dosimetry of ^{125}I brachytherapy sources,'' Med. Phys. **15**, 695–701 (1998).
[6] R. Waksman, ''Intercoronary radiation before stent implantation inhibits neointima formation in stented porcine coronary arteries,'' Circulation **92**, 1383–1386 (1995).
[7] B. R. Thomadsen, E. G. Hendee, B. R. Paliwal, L. A. DeWerd, and T. R. Mackie ''Evaluation of solid phantom materials for dosimetric measurements with beta emitters,'' Poster presentation at Advances in Cardiovascular Radiation Therapy II, Washington, DC (1998).
[8] M. Heydarian *et al.*, ''Evaluation of a PTW diamond detector for electron beam measurements,'' Phys. Med. Biol. **38**, 1035–1042 (1993).
[9] S. Vatnitsky and H. Jarvinen, ''Application of a natural diamond detector for the measurement of relative dose distributions in radiotherapy,'' Phys. Med. Biol. **38**, 173–184 (1993).
[10] C. G. Soares, D. G. Halpern and C. K. Wang, '' Calibration and characterization of beta-particle sources for intravascular brachytherapy,'' Med. Phys. **25**, 339–345 (1998).
[11] S. Kondo and M. L. Randolph, ''Effect of finite size of ionization chambers on measurements of small photon sources,'' Radiat. Res. **13**, 37–60 (1960).